

Electronic Supplementary Information

Hierarchical Micro/Nano-Structured Titanium Nitride Spheres as High-Performance Counter Electrode for a Dye-Sensitized Solar Cell

Xiaoying Zhang,^{a,b,‡} Xiao Chen,^{a,‡} Shanmu Dong,^{a,b} Zhihong Liu,^a Xinhong Zhou,^c Jianhua Yao,^a Shuping Pang,^a Hongxia Xu,^a Zhongyi Zhang,^{a,b} Lanfeng Li,^{a,c} Guanglei Cui^{*a}

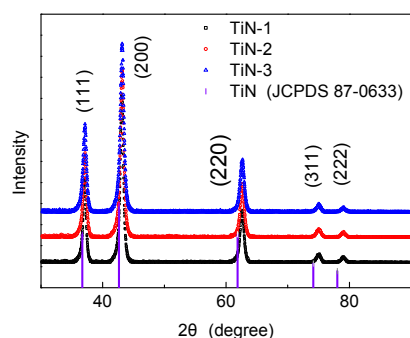


Fig. S1 XRD patterns of three particle sizes of hierarchical micro/nano-TiN spheres.

Fig. S1 presents that XRD patterns of the resultant samples. All the diffraction peaks can be indexed to cubic TiN (JCPDS 87-0633), belonging to the space group Fm3m. No obvious evidence of rutile or anatase TiO₂ can be found in the XRD pattern, which exclude the presence of TiO₂. Similar to our previous work, the diffraction peaks of hierarchical micro/nano-TiN shift to higher angles, which indicates a partial formation of TiN-TiO solid solution and nonstoichiometric TiN_x.¹ Furthermore, no obvious broadening of the diffraction peaks is observed in the samples with decreasing spheres size. It is confirmed that hierarchical micro/nano-TiNs are made up of densely packed similar sizes of primary nanoparticles and it is consistent with microscopy characterizations.

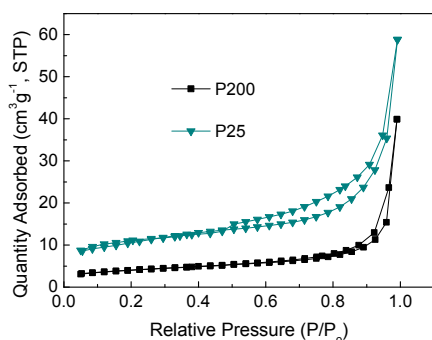


Fig. S2 Nitrogen-adsorption and desorption isotherms of P25 and P200.

As shown in Fig. S2, the N₂ adsorption-desorption curves of P25 and P200 have been carried out to evaluate the porosity and the surface areas of P25 and P200 is 36.6 and 14.0 m²g⁻¹, respectively.

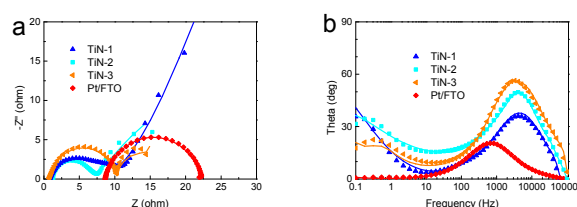


Fig. S3 Impedance spectra of the symmetric cells with two identical counter electrodes (a) Nyquist plots and (b) Bode phase plots. The symbols and lines correspond to the experimental and simulated data, respectively.

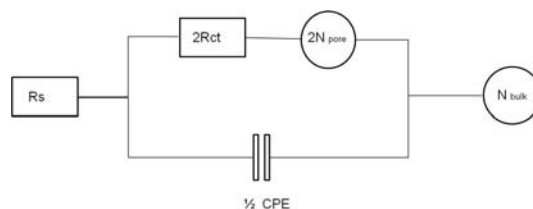


Fig. S4 The conventional equivalent circuit of the symmetric cell. R_s: series resistance; R_{ct}: charge transfer resistance of one electrode; N_{bulk}: Nernst diffusion impedance between the electrodes; CPE: constant phase element of one electrode, N_{pore}: Nernst diffusion impedance within electrode pores.

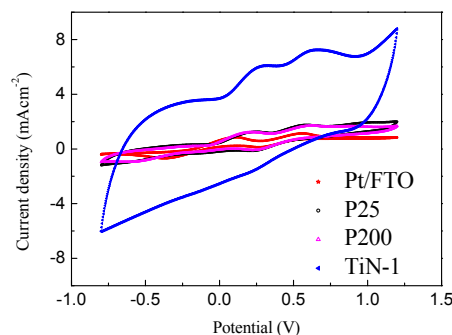


Fig. S5 Cyclic voltammograms of P25, P200, TiN-1 and Pt/FTO electrode at a scan rate of 20 mV s⁻¹ in 10 mM LiI, 1 mM I₂ acetonitrile solution containing 0.1 M LiClO₄ as the supporting electrolyte.

As shown in Fig. S5, P25 and P200 led to similar results, even if P25 hold bigger surface area. There could be ascribed to two reasons: 1) the aggregate of P25 sacrifices portion surface area; 2) abundant grain boundaries limit the electron-transport. As

for TiN-1, the current baseline is obviously high which is similar to the reported mesoporous carbon, owing to the generation of enormous active interface are

as.² That can be partly attributed to the double layer capacitance characteristic, which confirmed the porous structure of hierarchical micro/nano-TiNs.³ Besides, in comparison with P-TiNs, hierarchical micro/nano-TiNs exhibit a higher peak current density, which indicating a faster reaction rate presented owing to a larger active surface.⁴

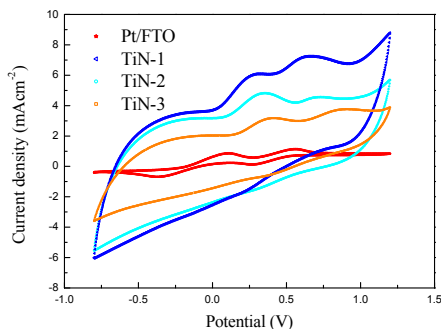


Fig. S6 Cyclic voltammograms of TiN-1, TiN-2, TiN-3 and Pt/FTO electrodes at a scan rate of 20 mVs⁻¹ in 10 mM LiI, 1 mM I₂ acetone/nitrile solution containing 0.1 M LiClO₄ as the supporting electrolyte.

Cyclic voltammogram (CV) was performed on hierarchical micro/nano-TiNs to evaluate their electrochemical performance. As shown in Fig. S6, for Pt electrode, two pairs of redox peaks are observed, which is similar to the previous literature.⁵ The relatively negative pair is attributed to reaction (1) (eq 1) and the positive one is attributed to reaction (2) (eq 2).⁶



In contrast, the cathodic peak of hierarchical micro/nano-TiNs referred to the reduction reaction of triiodide ions is absent, and instead there is a downward slope in the range from 0 V to 0.5 V. This phenomenon is also observed in carbon material and other inorganic materials.⁷⁻⁹ In addition, the formal potential shifts more positively for hierarchical micro/nano-TiNs, which might give rise to the gain of V_{OC}.¹⁰⁻¹²

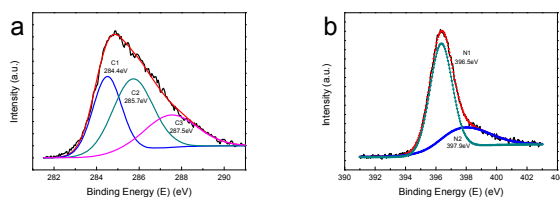


Fig. S7 XPS spectra and curve fitting of C 1s spectra (a) and N 1s (b) of TiN-3.

Fig. S7a exhibits three peaks by curve fitting of the C 1s spectrum of TiN-3. The peak at 284.4 eV is related to amorphous C, while the two weak peaks located at 285.7 and 287.5 eV reflect the different bonding structures of the C-N bonds, corresponding to the N-sp²C (C2) and N-sp³C bonds (C3), respectively.^{13, 14} The N 1s peak can also be split into two peaks as shown in Fig. S7b. The major N 1s peak at 396.5 eV is typical

for nitrogen shifts in metal nitrides and oxynitrides.¹⁵⁻¹⁷ The smaller intensity N 1s peak at 397.9 eV is related to C-N.^{18, 19}

An additional measurement was performed to qualitatively examine the mechanical adhesion of the hierarchical micro/nano-TiNs. The adhesive tape peel test was taken by sticking a Unipex adhesive tape on the hierarchical micro/nano-TiNs film and then peeling off the tape.²⁰ It was found that the adherence to the substrates was adequate for good mechanical stress during the cell manufacturing.

Table S1 Fitted electrochemical parameters from Electrochemical Impedance Spectra (EIS)

sample	R _s (Ωcm ²)	C (F)	R _{ct} (Ωcm ²)
TiN-3	0.65	2.54E-05	5.49
TiN-2	0.77	2.08E-05	3.81
TiN-1	0.84	2.16E-05	3.67
P25	0.29	7.28E-06	10.36
P200	0.41	7.37E-06	3.97
Pt foil	0.15	6.56E-05	2.62

Table S2 Elemental Composition of three different particle sizes of hierarchical micro/nano-TiNs

samples	N%	C%
TiN-1	18.29 ± 0.03	0.641 ± 0.06
TiN-2	17.1 ± 2.31	0.088 ± 0.02
TiN-3	16.92 ± 1.24	0.111 ± 0.01

Notes and references

- ¹ Qingdao Institute of Bioenergy and Bioprocess Technology, Chinese Academy of Sciences, Qingdao, 266101, P. R. China
² Graduate School of the Chinese Academy of Sciences, Beijing, 100080, P. R. China
³ Qingdao University of Science and Technology, Qingdao, 266101, P. R. China

China

† These authors contributed equally to this work.

* Corresponding author. E-mail: cuiql@qibebt.ac.cn

- ¹ S. Dong, X. Chen, L. Gu, X. Zhou, H. Xu, H. Wang, Z. Liu, P. Han, J. Yao, L. Wang, G. Cui and L. Chen, *ACS appl. Mater. interfaces*, 2011, **3**, 93-98.
² M. X. Wu, X. Lin, T. H. Wang, J. S. Qiu and T. L. Ma, *Energy Environ. Sci.*, 2011, **4**, 2308-2315.
³ D. Choi and P. N. Kumta, *J. Electrochem. Soc.*, 2006, **153**, A2298-A2303.
⁴ Q. B. Meng, Z. Huang, X. H. Liu, K. X. Li, D. M. Li, Y. H. Luo, H. Li, W. B. Song and L. Q. Chen, *Electrochem. Commun.*, 2007, **9**, 596-598.
⁵ D. Y. Kim, S. S. Kim, Y. C. Nah, Y. Y. Noh and J. Jo, *Electrochim. Acta*, 2006, **51**, 3814-3819.
⁶ A. I. Popov and D. H. Geske, *J. Am. Chem. Soc.*, 1958, **80**, 1340-1352.
⁷ M. Wu, X. Lin, A. Hagfeldt and T. Ma, *Angew. Chem. Int. Ed.*, 2011, **50**, 3520-3524.
⁸ G. R. Li, F. Wang, Q. W. Jiang, X. P. Gao and P. W. Shen, *Angew. Chem. Int. Ed.*, 2010, **49**, 3653-3656.

- 9 M. Wu, X. Lin, A. Hagfeldt and T. Ma, *Chem. Commun.*, 2011, **47**, 4535-4537.
- 10 K. Imoto, K. Takahashi, T. Yamaguchi, T. Komura, J. Nakamura and K. Murata, *Sol. Energy Mater. Sol. Cells*, 2003, **79**, 459-469.
- 5 11 Z. Ning, Y. Fu and H. Tian, *Energy Environ. Sci.*, 2010, **3**, 1170-1181.
- 12 M. L. Rosenbluth and N. S. Lewis, *J Phys Chem-Us*, 1989, **93**, 3735-3740.
- 13 S. Delpeux, F. Beguin, R. Benoit, R. Erre, N. Manolova and I. Rashkov, *Eur. Polym. J.*, 1998, **34**, 905-915.
- 10 14 J. C. Lascovich, R. Giorgi and S. Scaglione, *Appl. Surf. Sci.*, 1991, **47**, 17-21.
- 15 J. Ning, H. J. Zhang, S. N. Bao, Y. G. Shen and Z. F. Zhou, *Physica B*, 2004, **352**, 118-126.
- 16 F. H. Lu and H. Y. Chen, *Thin Solid Films*, 1999, **355**, 374-379.
- 15 17 B. M. Biwer and S. L. Bernasek, *Surf. Sci.*, 1986, **167**, 207-230.
- 18 J. Lahaye, G. Nanse, A. Bagreev and V. Strelko, *Carbon*, 1999, **37**, 585-590.
- 19 H. Schmiers, J. Friebe, P. Streubel, R. Hesse and R. Kopsel, *Carbon*, 1999, **37**, 1965-1978.
- 20 20 L. K. Kurihara, G. M. Chow and P. E. Schoen, *Nanostruct. Mater.*, 1995, **5**, 607-613.